Published in final edited form as:
Neuroimage. 2006 January 15; 29(2): 368–382. doi:10.1016/j.neuroimage.2005.08.065.

A temporal comparison of BOLD, ASL, and NIRS hemodynamic responses to motor stimuli in adult humans

T.J. Huppert[a,*], **R.D. Hoge**[b], **S.G. Diamond**[b], **M.A. Franceschini**[b], and **D.A. Boas**[b]

a*Harvard Medical School- Graduate Program in Biophysics, Massachusetts General Hospital, Charlestown, MA 02129, USA*

b*Athinoula A. Martinos Center for Biomedical Imaging, Massachusetts General Hospital, Charlestown, MA 02129, USA*

Abstract

In this study, we have preformed simultaneous near-infrared spectroscopy (NIRS) along with BOLD (blood oxygen level dependent) and ASL (arterial spin labeling)-based fMRI during an event-related motor activity in human subjects in order to compare the temporal dynamics of the hemodynamic responses recorded in each method. These measurements have allowed us to examine the validity of the biophysical models underlying each modality and, as a result, gain greater insight into the hemodynamic responses to neuronal activation. Although prior studies have examined the relationships between these two methodologies through similar experiments, they have produced conflicting results in the literature for a variety of reasons. Here, by employing a short-duration, event-related motor task, we have been able to emphasize the subtle temporal differences between the hemodynamic parameters with a high contrast-to-noise ratio. As a result of this improved experimental design, we are able to report that the fMRI measured BOLD response is more correlated with the NIRS measure of deoxy-hemoglobin ($R = 0.98$; $P < 10^{-20}$) than with oxy-hemoglobin ($R = 0.71$), or total hemoglobin ($R = 0.53$). This result was predicted from the theoretical grounds of the BOLD response and is in agreement with several previous works [Toronov, V.A.W., Choi, J.H., Wolf, M., Michalos, A., Gratton, E., Hueber, D., 2001. "Investigation of human brain hemodynamics by simultaneous near-infrared spectroscopy and functional magnetic resonance imaging." Med. Phys. 28 (4) 521–527; MacIntosh, B.J., Klassen, L.M., Menon, R.S., 2003. "Transient hemodynamics during a breath hold challenge in a two part functional imaging study with simultaneous near-infrared spectroscopy in adult humans." NeuroImage 20 1246– 1252; Toronov, V.A.W., Walker, S., Gupta, R., Choi, J.H., Gratton, E., Hueber, D., Webb, A., 2003. "The roles of changes in deoxyhemoglobin concentration and regional cerebral blood volume in the fMRI BOLD signal" Neuroimage 19 (4) 1521– 1531]. These data have also allowed us to examine more detailed measurement models of the fMRI signal and comment on the roles of the oxygen saturation and blood volume contributions to the BOLD response. In addition, we found high correlation between the NIRS measured total hemoglobin and ASL measured cerebral blood flow ($R = 0.91$; $P < 10^{-10}$) and oxy-hemoglobin with flow ($R = 0.83$; $P < 10^{-05}$) as predicted by the biophysical models. Finally, we note a significant amount of cross-modality, correlated, inter-subject variability in amplitude change and time-to-peak of the hemodynamic response. The observed co-variance in these parameters between subjects is in agreement with hemodynamic models and provides further support that fMRI and NIRS have similar vascular sensitivity.

*Corresponding author. *E-mail address:* E-mail: thuppert@nmr.mgh.harvard.edu (T.J. Huppert).

Keywords

Near-infrared spectroscopy; BOLD; ASL; Multimodality comparison

Introduction

Similar to its fMRI counterpart, near-infrared spectroscopy (NIRS) is a non-invasive method for studying functional activation through monitoring changes in the hemodynamic properties of the brain (Villringer et al., 1993; Hoshi and Tamura, 1993). However, unlike the commonly used BOLD (blood oxygen level dependent) based fMRI techniques, which derive contrast from the paramagnetic properties of deoxy-hemoglobin, NIRS is based on the intrinsic optical absorption of blood. As a result, NIRS has the ability to simultaneously record not only concentration changes in deoxy-hemoglobin (HbR) but in oxy-hemoglobin (HbO) and total hemoglobin (HbT) as well. In addition, unlike the majority of commonly used fMRI techniques, which typically have an intrinsically and instrumentation limited acquisition rate, the temporal resolution of hemoglobin detection with NIRS is not acquisition limited and can be up to hundreds of hertz, much faster then the hemodynamic response itself. In this respect, NIRS potentially provides a more complete temporal picture of brain hemodynamics compared with fMRI but suffers the drawbacks of lower spatial sensitivity and is limited by depth of light penetration in adult humans (0.5–2 cm) (Fukui et al., 2003). However, because of its complimentary informational content, NIRS is beginning to be experimentally combined synergistically with fMRI methods such as BOLD and arterial spin labeling (ASL). This was recently demonstrated by Hoge et al. (2005), where such a synergistic approach allowed for a direct calculation of the cerebral metabolic rate of oxygen metabolism ($CMRO_2$) with independently measured blood flow, volume, and hemoglobin oxygen saturation information. However, as such techniques continue to be developed, it is important to first establish the proper controls in order to understand the relationships between these methods and aid in the proper interpretation of such results.

One such control measurement for this purpose is the common measurement of HbR offered between the fMRI-BOLD signal and NIRS. The BOLD response is thought to reflect localized, relative changes in HbR levels (Kwong et al., 1992; Ogawa et al., 1992). Such MRI signal changes arise from susceptibility changes due to changes in local quantities of paramagnetic HbR, which give rise to shortening of the T_2 relaxation time of water molecules as they migrate through these regions. This change in relaxation times (ΔR_2^*) in turn gives rise to the changes in signal intensity, which underlie the BOLD response. Thus, one would expect to find a correlation both temporally and spatially between BOLD changes and NIRS measured total deoxy-hemoglobin. Accordingly, this common measurement potentially provides a basis for the cross-validation of both techniques. However, this comparison also provides further insight into measurement models of the BOLD signal, which suggest that the BOLD signal depends not only on the total deoxy-hemoglobin content of the tissue but also on venous inter-vascular oxygen saturation (Ogawa et al., 1992, 1993; Buxton et al., 1998).

In recent years, a number of research studies have attempted to examine the validity of this model by exploring the temporal correspondence between the NIRS and BOLD-fMRI recorded hemodynamic responses (Kleinschmidt et al., 1996; Punwani et al., 1998; Toronov et al., 2001, 2003; Strangman et al., 2002; Chen et al., 2003; Siegel et al., 2003). While qualitatively these results have supported a generalized spatial and temporal correspondence, detailed quantitative analysis of this relationship has produced mixed conclusions. In most cases, these reports have shown a very good correlation between fMRI and NIRS, but only a few have shown the correlation between HbR and BOLD to be better then that between HbO and BOLD as would be expected from models of the BOLD response (Toronov et al., 2001, 2003;

MacIntosh et al., 2003). The majority of this previous work has found either a slightly better correlation with HbO (Yamamoto and Kato, 2002; Strangman et al., 2002) or showed general agreement but did not comment on which hemoglobin species was most correlated to the BOLD response (Punwani et al., 1998; Chen et al., 2003). This issue has remained experimentally controversial for a few reasons. First, previous work suffered from a low contrast-to-noise ratio in the NIRS measurements along with the problem of absorption cross-talk between oxyand deoxy-hemoglobin. Recently, a number of groups have addressed this issue through analysis of the proper wavelength choices and partial path-length corrections (Yamashita et al., 2001; Strangman et al., 2003; Sato et al., 2004). This has led to improvements in the detection and discrimination of the hemodynamic response as reviewed by Boas et al. (2004). Secondly, most of this previous work has explored the hemodynamic response using functional paradigms with long periods of activation. The use of these longer paradigms, while giving large signal amplitude changes, fails to emphasize the subtle temporal differences between HbR and HbO, which are seen primarily in slight differences in the transition periods of each response. For the sustained task, the levels of both HbO and HbR quickly reach a steady state after only several seconds and generally remain at a plateau for the duration of the task. Thus, during a long task, the hemodynamic responses for both HbR and HbO are almost identical with the exception of only a short transient time at the beginning and end of the response. Since longer stimulus duration allows fewer repetitions of the task, these measurements become very susceptible to individual trial variance, which makes the already small difference in the time courses of HbO and HbR even more difficult to distinguish. When factored in with the additional problem of the inherent low temporal resolution of fMRI acquisition of these previous studies, which was itself on the order of the HbO:HbR time difference or greater, we can explain why previous multimodality studies have struggled to definitively distinguish between HbO and HbR signals when compared to BOLD.

In this study, we compared the temporal dynamics of the NIRS and fMRI hemodynamic response functions, aided by the methodological improvements of late. These have allowed us to address and surmount many of the issues of previous work. Here, we used an event-related paradigm with a short 2-s finger-tapping task to increase the number of activation periods and consequently the contrast-to-noise ratio in our estimate of the hemodynamic response function. This type of approach also focuses on the transient periods of hemoglobin change rather than the steady-state behavior allowing us to better highlight the differences between HbO and HbR. Combined with better temporal resolution fMRI measurements, which were afforded by a higher field magnet (3T) and again the event-related paradigm, this experimental design has allowed the measured hemodynamic responses in simultaneously acquired NIRS, BOLD and ASL-fMRI to be compared at 2 Hz temporal resolution. In addition, this is the first experiment specifically designed to examine the temporal relationship between ASL-fMRI and NIRS, a comparison that further strengthens the cross-validity of these approaches. Here, we report strong correlation between the modalities in terms of the expected analogous parameter pairs: HbR with BOLD and blood flow with blood volume. These relationships hold true for both group and individual analysis, despite a large degree of inter-subject variance in response time-to-peak. Thus, these data also demonstrate evidence for large physiologically based inter-subject differences in the dynamics of the hemodynamic response, which could have significant impact on the interpretation of group comparisons.

Methods

Subjects

In this study, we enrolled 11 healthy, right-handed subjects (8 males, 3 females). The subjects were 20–60 years old (mean 31 ± 10.5). The Massachusetts General Hospital Institutional Review Board approved the study, and all subjects gave written informed consent. For BOLD-

NIRS comparisons (study I), a total of 6 subjects were scanned. One subject failed to show any significant activation in both modalities and thus was excluded from further data analysis. The remaining five subjects (4 males, 1 female) all showed significant activation in both modalities. In the ASL-NIRS experiments (study II), again a total of 6 subjects were scanned. One of these subjects had to be excluded because of an extremely poor signal-to-noise ratio in the NIRS measurement due to poor coupling of the probe to the head. The remaining five subjects (4 males, 1 female) were included in the full analysis. One subject was repeated for both studies (subject B/F).

Protocol

Prior to placement into the bore of the MRI scanner, subjects were briefed on the details of the finger-tapping task. During data acquisition, subjects were instructed to watch a visual display from a laptop computer, which was projected from the back of the scanner room onto a screen in the bore of the magnet and was visible from a mirror mounted on the top of the MR head-coil above the subject's eyes. On this display was shown the text "STOP" or "GO". For the duration of the "GO" visual cue, subjects were instructed to sequentially tap their thumb and fingers on their right hand at a self-paced rate (approximately 2–3 Hz). After 2 s, the "GO" text was changed to the "STOP" command, at which time the subjects were instructed to stop tapping and keep their hand relaxed. Aside from the finger-tapping, subjects were otherwise instructed to remain motionless for the duration of the scanning session.

During the scan, the inter-stimulus interval between finger-tapping periods was psuedo-randomly chosen and optimized to provide the uniform temporal coverage necessary for deconvolution with a 500-ms time step (Dale, 1999). The length of the inter-stimulus interval (ISI) ranged between 4 and 20 s with an average inter-stimulus interval period of 12 s. A minimum ISI of 4 s was chosen to avoid the non-linear effects of the hemodynamic refractory period (Cannestra et al., 1998). The timing of the stimulus presentation was synchronized with the MR image acquisitions and generated with a custom written Matlab script (Mathworks, Sherborn, MA). Each run lasted 6 min and consisted of between 27 and 32 stimulus periods. This was repeated 4–6 times for each subject during the course of one scan session (approximately 90 min) for both the ASL and BOLD measurements. The experimental procedure, subject instructions, and stimulus parameters were identical for both the BOLD and ASL functional scans.

In order to verify subject compliance to the desired finger-tapping task, a fiber optic sensor was fixed to the subjects' thumb and forefingers and recorded simultaneously with NIRS and fMRI measurements. This sensor was placed in a "natural" position to avoid the subject from being required to actively tap on the sensor. These independent measurements were later compared to the synchronization pulse from the MR scanner to access subject compliance and estimate variance in subject response time and tapping rate. Unfortunately, due to technical problems, these values are reliably available for only five of the subjects.

NIRS acquisition and processing

In these experiments, we used a multichannel continuous-wave optical imager (CW4) to obtain the measurements as previously described (Franceschini et al., 2003). This instrument was developed jointly between the Photon Migration Lab at the Athinoula A. Martinos Center for Biomedical Imaging/Massachusetts General Hospital and TechEn Inc. (Milford, MA). The NIRS imager has 18 lasers – 9 lasers at 690 nm (18 mW) and 9 at 830 nm (7 mW) – and 16 detectors of which only 4 source positions (2 wavelengths each) and 8 detectors were used here. Laser wavelengths were chosen to maximize the contrast-to-noise ratio of the measurement (Yamashita et al., 2001; Sato et al., 2004), while minimizing the cross-talk error between the two hemoglobin species at 690 nm and 830 nm (18 mW and 7 mW respectively)

(Uludag et al., 2002, 2004; Strangman et al., 2003). The partial path-length correction to the Modified Beer–Lambert equation is similar at these two wavelengths determined within the uncertainty of the Monte Carlo methods used (Strangman et al., 2003). While not completely eliminating the possibility of cross-talk in the separation of hemoglobin species, this choice of wavelength pair was used to minimize such errors, which arise as a result of different light paths for the two wavelengths.

A master clock generates 18 different frequencies between 4 and 7.4 kHz in approximately 200 Hz steps, which are used to drive the individual lasers with current stabilized, square-wave, amplitude modulation. This enables unique identification of each source by demodulation against the known carrier frequencies on each detector channel. For detectors, the imager employs 16 avalanche photodiodes (APD's, Hamamatsu C5460-01), each of which is digitized at approximately 40 kHz. A bandpass filter follows each APD module with a cut-on frequency of approximately 500 Hz to reduce 1/f noise and the 60 Hz room light signal and a cut-off frequency of approximately 16 kHz to reduce the third harmonics of the square-wave signals. The signal is then passed to a programmable gain stage, which is used to match the signal levels with the acquisition level on the analog-to-digital converter within the computer. A digital demodulation and low-pass filter is used off-line to separate the individual source signals on each detector channel. This is done via a seven-pole infinite-impulse-response filter with a 10 Hz band pass frequency centered on the 18 carrier frequencies generated by the master clock.

The NIRS probe was made from flexible plastic strips with plastic caps inserted in it to hold the ends of the 10-m source/detector fiber optic bundles. The probe consisted of two rows of four detector fibers and one row of four source fibers arranged in a rectangular grid pattern and spaced 2.9 cm between nearest neighbor source detector pairs as shown in Fig. 1. This plastic probe was then secured to the subject's head centered over the contra-lateral primary motor cortex (M1) via Velcro straps and foam padding. The 10-m fibers were run through the magnet bore to the back of the scanner and through a port into the control room where they were connected to the NIRS instrument. The CW4 instrument was then run from the MR control room.

After collection, demodulation and low-pass filtering at a 10 Hz bandwidth to separate individual source contributions, the data were further processed using a custom Matlab data analysis program (HomER: available for public download and use at http://www.nmr.mgh.harvard.edu/PMI/). Signals were further low-pass filtered at 0.8 Hz using a zero-phase forward and reverse digital filter to remove the heart signal. Changes in optical density for each source detector pair were then high-pass filtered with a 1/30 Hz drift correction and finally converted to change in hemoglobin concentrations using the modified Beer–Lambert relationship with a differential path-length correction of 6 and a partial volume correction of 50 for both wavelengths (Strangman et al., 2003). At the two wavelengths used in this study, the corrections for the each wavelength are very similar (Uludag et al., 2002; Strangman et al., 2003) and were empirically verified to not have a significant impact on the calculation of normalized responses nor final correlations with the fMRI responses by allowing the partial path-length values to independently vary ±20% and repeating the correlation analysis (data not shown). From concentration data, the individual subject hemodynamic responses were calculated using an ordinary least-squares (OLS) linear deconvolution and implemented within the HomER program (e.g., Serences, 2004). No nuisance variable polynomial trends were fit in the linear regression, since these had been already removed by the low and high-pass filtering steps. For both the fMRI and NIRS time-series analysis, no fixed canonic responses (i.e., Gaussian or gamma variants) were assumed, which allowed comparison of the response functions from both modalities without introducing errors that might have arisen from such assumed response functions. Epoch timing was synchronized to the MRI images so that subject response times were kept constant between the fMRI and NIRS.

Regions of time showing significant motion artifacts (as clearly evidenced by extremely large and sudden perturbations in the measurement time course) were rejected from the analysis. The impulse response functions were then averaged across all runs for each subject taken within the same scan session for each source detector pair. To compare the impulse responses of the entire activation area, a region of interest average for each subject was calculated from the average of all nearest neighbor source detector pairs, which showed statistically significant activation based on the calculated T statistic for each channel ($P < 0.05$). The responses were additionally averaged together to generate the grand average of all five subjects for each study. It should be noted that although the region-of-interests were chosen here based on the inclusion of only significant channels, inclusion of all channels did not change the results qualitatively and only introduced a partial volume error that affected the quantitative results but did not appreciably affect the line–shapes, timing, nor correlations with the fMRI. Since the spatial resolution of neither the fMRI nor NIRS was sufficient to distinguish between motor and sensory activation, both regions were potentially included in this analysis.

fMRI acquisition and processing

For study I, BOLD-fMRI measurements were preformed using a 3 T Siemens Allegra MR scanner (Siemens Medical Systems, Erlangen Germany). Data were taken with an (gradient) echo EPI sequence [TR/TE/θ = 500 ms/30 ms/90°] with five 6-mm slices (1-mm spacing) and 3.75-mm in-plane spatial resolution. Structural scans were performed using a T1-weighted MPRAGE sequence [1 × 1 × 1.33-mm resolution, TR/TE/θ = 2.53 s/3.25 ms/7°].

To calculate the BOLD-based hemodynamic response functions, the functional images were first motion corrected (Cox and Jesmanowicz, 1999) and spatially smoothed with a 6-mm Gaussian kernel. The response functions were then calculated by an ordinary least-squares linear deconvolution. A third order polynomial was included to remove drift effects. As with the NIRS analysis, the hemodynamic response was estimated without assumptions of fixed canonical responses. For each subject, the effect and standard deviation maps were input to a mixed effects analysis (target degrees of freedom = 100) to generate a map of T-statistic used to identify regions of significant response (Worsley and Friston, 1995). Each T-map was thresh-held ($P < 0.01$), and significant pixels were manually selected under the NIRS probe based on the fiducial markers (as shown in Fig. 2). Note that no voxels with changes greater then 17% from baseline were identified within the ROI. As with the NIRS regions-of-interest, no specific attention was paid to separating sensory and motor effects.

For study II, ASL-fMRI was carried out at 3 T (same scanner as study I) using PICORE labeling geometry (Wong et al., 1997) with Q2TIPS saturation (Luh et al., 1999) to impose a controlled label duration. A post-label delay of 1400 ms and label duration of 700 ms were used, with repetition and (gradient) echo times of 2 s and 20 ms respectively [θ = 90°]. The PICORE labeling scheme allowed collection of BOLD signals using the control phase of the acquisition. EPI was used to image five 6-mm slices (1-mm spacing) with 3.75-mm in-plane spatial resolution. Structural scans were also performed with the same scan prescriptions as study I.

Although the original image acquisition was at 2 s, the stimulus had been jittered evenly on a 500-ms time step, which allowed for the response to be calculated at 2 Hz, albeit with lower signal-to-noise. To estimate the flow response, the ASL functional scans were first separated into the control and negatively labeled tag images. These traces were then independently interpolated to up-sample the data points to 2 Hz using a cubic spline model (de Boor, 1978). Subtracting each negatively labeled tag scan from the immediately subsequent control scan generated the flow image series. This flow series was then deconvolved and the region of interest average calculated similar to its calculation for the BOLD response. Since the intermixed control images recorded the BOLD response, this series of images allowed the

BOLD response function to be calculated from the study II data as well and is included in the results.

Results

The event-related finger-tapping task resulted in the expected hemodynamic changes in the primary motor and sensory cortices, which was detected in all ten subjects used between the two studies. Fig. 3 shows a typical (ROI) hemodynamic response function as recorded by the NIRS instrument for one such subject (D).

Similar to previous results, we noted a delay between the HbO, HbT, and HbR responses. The average lag between peak HbR and HbO (HbT) responses was approximately 2.0 s (2.1 s). These results were similar to those previously reported for the same task (Jasdzewski et al., 2003). This HbR lag was observed for all subjects in both studies, although the exact timing and lag length varied considerably between subjects between almost 0 and 3.6 s. The time-to-peak of each of these parameters is presented in Table 1, which again showed a wide variability. The concentration changes in HbO, HbT, and HbR averaged over this entire experiment from the 10 subjects were found to be 7.9 ± 1.8 μM, 6.6 ± 1.5 μM, and −2.2 ± 1.4 μM respectively (average ± SD), with assumed partial volume and path-length corrections as described above. Assuming baseline conditions of 25 μM and 60 μM for HbR and HbO respectively (Torricelli et al., 2001), this represents a 13.2%, 7.8%, and −8.8% change [HbO/HbT/HbR respectively]. The average BOLD and ASL change were 2.6 ± 1.3% and 28.2 ± 11% respectively.

Study I—BOLD/NIRS

Individual subject measurements were gathered and processed as described in the previous section. For the simultaneous BOLD/NIRS recordings, five of the six subjects tested showed significant activation. The NIRS data for the sixth subject had a very low signal-to-noise ratio and contained numerous motion artifacts. This subject failed to show any localized significant activation in the BOLD *t* statistics maps nor any significantly activated NIRS source detector pairs. As a result, this subject's data were excluded from further analysis. The traces for the simultaneously acquired hemoglobin and BOLD data for the remaining five subjects are shown in Fig. 4. Data have been normalized to the maximum change, and the HbR traces have been inverted to allow better visual comparison.

To further examine these relationships, we averaged the normalized responses from all five subjects (shown in Fig. 5). Similar to the group averaged HbR response, the Δ(1/BOLD) ($\sim\Delta R_2$) response also peaks at around 6.3 ± 0.8 s and closely follows the HbR time course for the time window up to about 12 s post-onset. As the result of a sizable inter-subject variance in the response times, the averaged response is broader then the individual responses as expected. In the subject averaged response, the HbO and HbT responses peaked at approximately 4.6 s and 4.5 s respectively.

To quantitatively examine the correlation between the BOLD and NIRS responses, we preformed a cross-correlation analysis with the averaged and individual subject results. The zeroth-lag Pearson's correlation coefficients, which are presented in Table 2, show highly significant correlation between the Δ(1/BOLD) and HbR responses in all individual subjects as well as the average across all five subjects. These values were all calculated over the time range of 0–15 s. In all but subject E, the HbR was the most significantly correlated with the BOLD signal. In fact, this discrepancy for subject E arises from the slight noise in the HbR signal in the time frame of 10–15 s post-stimulus in that subject. For this subject, if only the time period from 0 to 10 s is instead used, the correlation between HbR and BOLD improves to $R = 0.84$ ($P < 3 \times 10^{-06}$) with $R = 0.56$ and 0.42 for HbO and HbT respectively ($P = 1 \times 10^{-01}$ and 6×10^{-02}). The overall correlation coefficients from all five subjects were then

calculated from a cross-correlation analysis using the ROI average response functions over the same time (0 –15 s). The correlation coefficients for HbO, HbT, and HbR to Δ1/BOLD are 0.71, 0.53, and 0.98 ($P = 1 \times 10^{-05}$, 2×10^{-03}, and 8×10^{-21}) respectively.

Finally, Fig. 6 shows parametric plots of the three hemodynamic parameters and the BOLD signal for all five individual subjects (top three plots) and the group average (bottom plots) for the time period up to 15 s post-stimulus. Deoxy-hemoglobin clearly shows much stronger linear correlation with the BOLD signal then the other two hemoglobin species, especially at larger contrast levels. The HbO an HbT response profiles have similar line–shapes to the HbR and BOLD responses but are shifted earlier in time, giving rise to the oval shaped plots in Fig. 6.

Study II—ASL/NIRS

In the second half of this study, we repeated the same motor task experiment preformed in study I, but this time, we compared the NIRS measurements against cerebral blood flow as measured by ASL based fMRI. Here, we were again able to compare the NIRS and fMRI measurements at 2 Hz by the use of the jittered stimulus timing and processing as described earlier. The NIRS measurements were consistent with those from the previous sessions, and again, we found that the HbR response was slightly lagged behind that of HbO and HbT (Table 1). This lag was consistent with the temporal difference between the BOLD and ASL responses, which were approximately 1–2 s apart. A similar temporal lag between BOLD and ASL has also been previously noted in other studies (Liu et al., 2000,Yang et al., 2000,Aguirre et al., 2002). As shown in Fig. 7 (individual responses) and Fig. 9 (group average) and the BOLD response again closely matched the HbR time course ($R = 0.81$; $P = 9 \times 10^{-08}$) and in agreement with our initial hypothesis, the HbO and HbT responses were found to be highly correlated with the ASL response ($R = 0.83$; $P = 5 \times 10^{-13}$ and $R = 0.91$; $P = 5 \times 10^{-12}$). In Fig. 8, we present the parametric plots of the ASL response against the three hemoglobin species for the individual (top three plots) and group data (bottom plots). Plots of the BOLD and hemoglobin responses in this study (data not shown) were similar to those presented in Fig. 6 for study I.

As shown in Table 3, in all five subjects used, the ASL measurement was more correlated with that of the NIRS HbO and HbT responses than with the HbR response; with all but one subject showing slightly higher correlation between the HbT and ASL responses. Again, four of the five subjects showed better correlation between HbR and BOLD then either HbO or HbT and BOLD. In subject F, a marginally better correlation was seen with HbO:BOLD. However, this difference was not significant ($P > 0.4$) in a *t* test of the *Z*-transformed Pearson's coefficients.

Discussion

Comparison of NIRS and BOLD measurements

In agreement with our initial hypothesis, the simultaneous NIRS and BOLD-fMRI measurements, as shown in Fig. 5 and Fig 9 and presented in Table 2 and Table 3, clearly show very close agreement between BOLD and HbR measurements. This relationship was found for the BOLD signals measured in both studies. In study I in particular, which had a better signal-to-noise ratio compared to the recorded BOLD signal from study II, we found a correlation value of $R = 0.98$ ($P < 8 \times 10^{-21}$) between the BOLD and NIRS measured HbR responses. We believe that this strong corroboration between the two modalities provides cross-validation that both techniques are measuring brain deoxy-hemoglobin dynamics. This provides strong support of both previous theoretical and experimental work supporting HbR changes as the origin of the BOLD signal and supports the ability of NIRS to measure hemodynamic changes within the brain.

Unlike many of the previous studies, we have shown that there is not only general agreement between the fMRI and NIRS in terms of observing a task-correlated signal change, but that correlation between BOLD and NIRS was more significantly for the HbR component. In this experiment, since we used a relatively short duration task and aided by the improvements in signal-to-noise afforded by our event-related design, the time courses for the HbT, HbO, and HbR parameters were clearly separated from each other. As a result of this temporal separation, we were able to show that the BOLD:HbR correlations were much stronger then the BOLD to HbO or HbT correlations ($P < 1 \times 10^{-05}$). Since the temporal lag between HbO and HbR is only about 2 s, this distinction would not have been as statistically significant had we used a long duration task, and as a result, we would not have been able to show such a significantly better correlation between HbR and BOLD. We believe this explains the discrepancies between this result and previous work which had course temporal resolution and found better correlation between BOLD and HbO presumably because HbO had a better signal-to-noise ratio than HbR (Yamamoto and Kato, 2002; Strangman et al., 2002).

Examination of BOLD model

In this study, we found significantly better correlation between the total deoxy-hemoglobin content per volume as recorded by the NIRS instrument (HbR) and the BOLD signal. Although this observation suggests that the BOLD signal is significantly more related to HbR then HbO or HbT, this does not refute the previous theoretical work which theorized that BOLD would vary with both the total deoxy-hemoglobin content and oxygen saturation, giving rise to the extra and intra-vascular signals respectively (Ogawa et al., 1992, 1993). The inter-vascular signal, which composes the majority of the BOLD signal at moderate field strengths (below 4T), arises from the interaction of water molecules directly with the deoxy-hemoglobin molecules within the veins (Ogawa et al., 1993) and varies linearly with the venous concentration of deoxy-hemoglobin (Li et al., 1998). The extra-vascular signal, which arises from magnetic susceptibility differences between the blood vessels and the surrounding tissues, depends on the total deoxy-hemoglobin content within a voxel. This signal becomes a larger component of the BOLD signal as field strengths increase (Obata et al., 2004). Thus, the BOLD signal would be expected to vary as a function of both oxygen saturation and blood volume (Ogawa et al., 1993; Buxton et al., 1998).

To test the possibility that the BOLD signal could be modeled as the linear superposition of volume and saturation effects, we decided to apply multiple linear regression of the BOLD signal with the NIRS parameters. Based on the measurement model presented by (Obata et al. 2004; Ogawa et al., 1993), the relative BOLD signal can be expressed in terms of the normalized fractional venous blood volume ($v = V/V_o$) and the normalized total deoxy-hemoglobin content ($q = V(1 - Y) / V_o(1 - Y_o)$; where Y is the oxygen saturation of the veins pool):

$$\frac{\Delta S}{S_o} \approx V_o \left[(k_1+k_2)(1-q) - (k_2 - k_3)(1-v)\right] \quad (1)$$

This model is testable with our data, since the q and v regressors can be approximated by the baseline normalized NIRS measured HbR and HbT parameters. Although the NIRS measure of total hemoglobin changes is not explicitly venous derived, as a first approximation, this allows us to consider this model without compartmentalizing the data into arterial and venous contributions. Future analyses will have to consider the effects of q and v from the different vascular compartments. For now, we used estimated baseline values of 25 μM and 85 μM for HbR and HbT respectively (Torricelli et al., 2001). The dimensionless parameters $k_{\{1,2,3\}}$ depend on the fMRI echo time (TE), baseline oxygen extraction, tissue composition, and magnetic field strength, while V_o is the baseline blood volume fraction. At 3 T, these values can be estimated to be $\{k_1 = 4.2\ (2.7); k_2 = 1.7\ (1.1); k_3 = 0.41\ (.30)\}$ for study I (TE = 30 ms)

and II (TE = 20 ms), based on values and equations presented in (Mildner et al., 2001). These theoretical values would predict a relative contribution from the NIRS measured HbR (q) and HbT (v) of 2.8:1 and 2.7:1 for studies I and II respectively. This ratio is given by $(k_1 + k_2) / (k_2 + k_3)$, which normalizes out the estimate of the volume fraction (V_o).

In Table 4, we present the model fit and calculated coefficient ratios for the two studies obtained through this multiregression analysis. As can be seen by the Pearson coefficients for each subject, there was only modest improvement compared to the original correlation with just HbR. Similar findings have previously been shown by Toronov et al. (2003). However, since both HbR and HbT are correlated to the BOLD signal and are themselves correlated to each other, this coefficient does not adequately describe the redistribution of the variance between the two regressors.

Using an analysis of variance approach, we calculated the partial F statistic values associated with the addition of the HbT regressor to a regression model of the BOLD signal already including HbR, i.e., F(BOLD,HbT|HbR) given in Table 4. This test, which follows a χ^2_{n-2} distribution, tests the null hypothesis of whether the coefficient multiplying HbT (i.e., $k_2 + k_3$) equals zero. With the exception of subject H, this test met a $P < 0.05$ criterion for the individual subjects and the group averages, suggesting that HbT explains a significant additional amount of the BOLD signal and accounts for roughly 36% of the variance in the BOLD signal based on partial-R^2 analysis in the average of both studies. To increase our confidence in the BOLD dependence on HbT, we performed a partial correlation analysis (Whittaker, 1990;Gather et al., 2002) between the three variables: HbR, HbT, and BOLD. We used this analysis to determine the correlation between BOLD and HbT controlling for the correlation of HbR and HbT. As shown in Table 4, the correlation between BOLD and HbT remains.

In addition to testing the statistical influence of changes in HbR and HbT on the BOLD, we can also estimate the ratio of the regression coefficients from Eq. (1). The ratio of the coefficients $(k_1 + k_2)/(k_2 + k_3)$ was found to be 4.2 ± 1.0 and 2.5 ± 1.4 [mean ± StdErr] for the five subjects in studies I and II respectively. In all cases, the sign of both the individual coefficients was positive, indicating positive relationship between BOLD and HbT. The theoretically predicted values for this ratio were 2.8:1 and 2.7:1 based on the previously cited values of $k_{\{1,2,3\}}$ and echo times. These results are in reasonable agreement with the expected values. Partial volume and/or errors in the estimate of the path length in the modified Beer–Lambert relationship affecting the absolute magnitude of the changes could account for this discrepancy.

Comparison of NIRS and ASL measurements

In study II, we further investigated the functional MRI and NIRS relationships by studying the correlation of ASL measured blood flow and the hemoglobin parameters measured by NIRS. Based on predictions of biomechanical models of the hemodynamic response (Buxton et al., 1998, Mandeville et al., 1999), we hypothesized that blood flow and total hemoglobin (blood volume) would be best correlated. Since we expect a fairly tight coupling between flow and volume, we expected that the onset and time-to-peak of these two variables would be very similar. In addition, since the majority fraction of the total hemoglobin is HbO, we expected HbO to also correlate with ASL, but because of washout and metabolic influences, we expected this correlation to be slightly weaker. Indeed, when we investigated the relationship between NIRS and ASL measured blood flow in study II, we found the expected significant correlation between HbO, HbT, and ASL that was predicted by our hypothesis. In all five subjects, these correlations where much more significant than that between the ASL and HbR responses (R = 0.13; P = 0.5), and in four of the five subjects, we found that HbT was slightly better correlated

with the ASL signal ($R = 0.91$; $P = 4 \times 10^{-12}$) than was the HbO response ($R = 0.83$; $P = 8 \times 10^{-08}$). The difference in lag times between the ASL and BOLD responses (2.2 ± 0.9 s) is similar to that between HbT and HbR as well as HbO and HbR. Previous fMRI work comparing perfusion and BOLD-based methods have also reported a similar temporal mismatch with perfusion traces peaking slightly prior to the BOLD response (Liu et al., 2000; Yang et al., 2000; Aguirre et al., 2002). Together with the findings from study I, these results provide further support for the hemodynamic origins and interpretation of the fMRI signals and support the use of NIRS as a functional brain imaging methodology.

In the group-average of these five subjects, we did notice that the ASL measurements appeared to have a more pronounced post-stimulus undershoot compared to HbT (blood volume). As shown in Fig. 9, the trace of CBF (ASL data) closely follows that of HbT for the first 6 s of the response but deviates after around 6 s as blood flow further undershoots below its baseline value. In these data, we do observe that HbO and HbT also undershoot their baseline values, however, not as markedly as the flow measurements. The possibility of a flow undershoot would suggest a mechanism to explain the HbT, HbO, and HbR (BOLD) undershoots as well. Similar flow undershoots have been previously noted in human visual cortex (V1) with ASL measurements (Hoge et al., 1999). These have also been observed during laser-Doppler flowmetry (LDF) measurements in rodents during vibrissal (Ma et al., 1996) and electrical fore-paw stimulation (Mandeville et al., 1999), although this undershoot in LDF measurements is usually attributed to the uncorrected under-estimation of flow at high volume levels (Mandeville et al., 1999). This possibility of a post-stimulus undershoot in flow and its implication on the interpretation of fMRI and NIRS measurements requires further investigation.

Inter-subject variability and interpretation

In this study, although we consistently noted the expected correlations between pair-wise parameters in individual and group averages, as demonstrated by Fig. 4 and Fig 7, we found a large degree of cross-modality correlated inter-subject variability in the shape and timing of the hemodynamic response. In some cases, the HbR and HbO/HbT traces were nearly simultaneous, peaking nearly opposite to each other. In other cases, the HbR response was well separated and delayed from the other hemoglobin time courses. The ASL and BOLD traces also showed a similar variability, and in almost all cases, the strong correlations between fMRI and NIRS parameters held despite this variability. This suggests that this variability is not the result of systematic measurement error (for example, the result of the MRI or NIRS acquisition protocol) but instead represents real physiological or anatomical differences underlying the hemodynamic response.

To first rule out the possibility of behavioral explanations for this variability, we noted that these inter-subject differences are not explained by physical task differences since tapping frequencies could be calculated for half (5) of the subjects and were found to be between 1.5–3 Hz (Avg = 2.4 ± 0.4 Hz) with no clear correlation between tapping frequency and latency of response nor magnitude of the response. Due to technical reasons, we could not calculate quantitative tapping frequency information for the remaining subjects. Subject D, in particular, had a very latent response compared to the other nine subjects with HbO/HbT not peaking until after over 7 s post-stimulus trigger. However, from the auxiliary finger-tapping sensor, it is clear that this subject was perfectly compliant with the task, and that his response time was comparable to the other subjects. The precise response times for each subject could not be extracted from the finger sensor recordings but could be estimated to be no more then several hundred milliseconds and not enough to explain the variation of several seconds seen in the response time-to-peaks.

Since this variability was correlated between the fMRI and NIRS measurements, we proposed that the source of this variability should have physiological or anatomical origins common to both modalities. Previous work has noted a similar inter-subject variability in the BOLD response under a number of different conditions. Such variability in the BOLD time-to-peak has been seen in both ROI analyses across subjects (Aguirre et al., 1998; Miezin et al., 2000) as well as regionally within subjects (Miezin et al., 2000). Previous fMRI literature has hypothesized that this variability in the latency of the BOLD response is the result of increased (gradient echo) fMRI sensitivity to the larger draining (pial) veins, which give rise to both a later response and have a higher contrast-to-noise ratio compared to smaller veins (Lee et al., 1995; Boxerman et al., 1995).

Similar to GE-fMRI, for NIRS, it is likely that larger pial veins (≤1 mm) give rise to larger, higher contrast signals (Liu et al., 1995). Liu et al. (1995) predicted that NIRS has uniform measurement sensitivity to blood vessels with diameters smaller then the optical absorption length (~1 mm for whole blood at 800 nm). While the signal-to-noise ratio to vessels in this size range is uniform, the hemodynamic contrast, which is the product of this measurement sensitivity and the magnitude of the response, would be expected to increase for increasing vessel diameter. Thus, the contrast-to-noise ratio of NIRS is likely to increase with vessel size up to approximately 1 mm in diameter, as these veins will have larger overall changes in hemoglobin concentrations. Since the venous sinuses and collecting veins are typically larger then the 1-mm absorption length, these vessels would be expected to have very little signal contribution to the NIRS measurements as they absorb the majority of traversing light (Liu et al., 1995). In this respect, we feel that both NIRS and GE-fMRI will have similar vascular contrast profiles and thus will be similarly weighted to the pial vessels within a region-of-interest average. This is further corroborated by our ASL:NIRS and BOLD:NIRS comparisons, which would generally not have been as correlated if NIRS and fMRI had significantly different vascular sensitivities.

We therefore speculate that the inter-subject variability in the time-to-peak of the response is the result of different vascular profiles between subjects. In the case of both the BOLD and NIRS-HbR measurements, which are both expected to be venous weighted, the larger veins will have a larger contrast-to-noise ratio. These areas will be more heavily weighted in an ROI average that is based on *P* value thresh-holding, as was used here. This results in temporal dynamics of the region-of-interest average that reflects the partial volume contributions of these larger draining veins. Thus, the higher the volume fraction of draining veins in the ROI, the response will be more latent and have greater amplitude. In contrast, NIRS measurements of HbO and HbT would be expected to have a greater weighting to the arterial compartments than HbR. The more downstream draining veins likely only exhibit oxygenation changes from washout effects and will likely not have blood volume changes that correlate with latency.

This hypothesis predicts a correlation between the timing and amplitude of the individual responses for HbR but not for HbT. As expected, we found that the overall time-to-peak of the response and the maximum amplitude change were highly correlated ($P < 0.05$) for HbR response (presented in Table 5). We also noticed a similar, but less statistically strong, trend for HbO as well. We found no such correlations in the relationship between time-to-peak of the response and HbT amplitude change ($P > 0.5$), which provides further support for this hypothesis as the larger downstream draining veins likely have little volume change. However, the possibility of a correlation cannot be discredited due to increased inter-subject variance of the response amplitudes arising from NIRS partial volume effects. Alternatively, we might hypothesize that differences in the baseline conditions (blood flow, volume, and oxygen saturation) could give rise to similar inter-subject variability. However, in that model, we would have expected to find a correlation between HbT amplitude change and time-to-peak.

Although these correlations are in line with our hypothesis that the inter-subject variability we noted in the hemodynamic responses might be due to increased sensitivity of both the BOLD and NIRS signals to larger blood vessels (up to 1 mm), the true source of this variability is still unknown. However, since this variability is found across both modalities, we believe that this represents actual physiological variability between subjects and should be further investigated in future studies. We would also like to point out that this inter-subject variability could have a potential impact on the use of group averaging in quantitative analysis of both NIRS and fMRI data, particularly in analysis where a single response line-shape is assumed for all subjects. This issue has been discussed as an area of concern in previous literature (Aguirre et al., 1998), and the finding that this variability carries across imaging modalities further strengthens this concern. In this study, we used a blind least-squares deconvolution for all the analysis in both the NIRS and fMRI and thus avoided the generalized canonical models that might influence the results in light of such variability.

Comparing hemodynamic amplitude changes between subjects

Although our results demonstrate significant correlation between the amplitude and latency of the hemodynamic response across subjects, some care must be taken to understand the validity of such amplitude comparisons. As pointed out by previous researchers (Uludag et al., 2002, 2004; Strangman et al., 2003), differing partial volume factors arising from the source detector positions relative to site of activation, depth of activation, scalp and skull thickness, and baseline optical properties can all potentially cause large variance in the NIRS estimate of amplitude changes between subjects when not controlled or modeled. Thus, probe placement as well as differing individual subject anatomy are sources of random variance in the partial volume effect. While this means that individual data is highly variant, this does not completely prevent inter-subject amplitude comparisons and analysis of the statistical trends in group averages. Instead, to compensate for this increased variance, more subjects' data are required in order to demonstrate statistical significance. Interestingly, in this experiment, we found statistically significant correlation ($P < 0.05$) between the response amplitude and latency with only 10 subjects. This finding suggests that such comparisons are not as fallacious as once suggested. Future improvements to characterize the partial volume factors based on anatomical information (Barnett et al., 2003) as well as the use of tomographic probe geometries to give more uniform spatial sensitivities (Boas et al., 2004) will likely further reduce this partial volume variance, improving such amplitude comparisons.

Comments on the generality of these results

In general, we expect that there should be a strong correlation between the BOLD and HbR responses. Based on our partial-regression analysis of the measurement model of the BOLD response suggested by Ogawa et al. (1993), we also found a small but significant contribution of blood volume. However, although this experimental design yielded convincing evidence for the correlation of these two methodologies and supported this measurement model, we must be cautious in drawing conclusions on the generality of these conclusions to other experimental situations. For example, while the correlation between BOLD and HbR should in general remain true, the details of this relationship will change depending on a number of experimentally defined or subject specific parameters particularly those which affect the BOLD measurement, such as echo sequence or field strength. For both NIRS and fMRI, the observed hemodynamic parameters such as blood volume, HbO, or HbR are spatial and temporally filtered versions of their true underlying changes in the brain. The BOLD signal, for example, is an indirect measurement of HbR, depending on details of the fMRI acquisition sequence, baseline properties of the brain, and vascular sensitivities with both extra and intravascular contributions (Boxerman et al., 1995). In general, these parameters and filters are not known and should not be expected to be identical between the NIRS and fMRI. As a result of this, although both methods may be functions of the same changes in underlying HbR, the measured

results may differ because the filter functions may differ. Since these vascular filters will depend on a number of factors including the acquisition scheme employed, it is possible that other echo, scan parameters, or even brain regions may yield slightly differing results.

Conclusions

The synergistic information content between the NIRS and fMRI methodologies provides an attractive possibility of future multimodality studies. It is clear that, although both methods measure aspects of the hemodynamic response, they do so using very different means. As a result, measurement sensitivity, data processing, and the very different physics of acquisition can all potentially play important roles in interpretation of these results. Vital to the correct interpretation of such multimodality studies, proper control experiments must be first preformed. In this study, the common measurement of HbR between the BOLD-fMRI and NIRS recordings provided one such control. Our results here show an extremely strong statistical correlation between these measurements ($P < 8 \times 10^{-21}$), which is supporting evidence for the cross-validity of such approaches. Our data also showed a significant partial contribution of HbT to the BOLD signal in each subject. This supports the BOLD measurement model proposed by Obata et al. (2004). In addition, based on biophysical models of the hemodynamic response, we had postulated that similar temporal dynamics between the ASL measured flow response and the NIRS measured HbT would provide a second means of this cross-validation. Again, in agreement with this hypothesis, we found this correlation to be significant ($P < 4 \times 10^{-12}$). We believe these results provide convincing evidence for the hemodynamic signal origin for both the fMRI and NIRS techniques. However, since this study only examined the temporal relationships between these methods, further work must be done to understand the spatial relations between the NIRS and MR imaging techniques.

Acknowledgments

We would like to thank Christiana Andre, Danny Joseph, and Elizabeth Alf for helping in organizing and performing the experimental sessions. T.J.H. is funded by the Howard Hughes Medical Institute predoctoral fellowship program. This work was supported by the National Institutes of Health (R01-EB002482, RO1-EB001954, and P41-RR14075).

References

Aguirre GK, Zarahn E, D'Esposito M. The variability of human, BOLD hemodynamic responses. NeuroImage 1998;8:360–369. [PubMed: 9811554]

Aguirre GK, Detre JA, Zarahn E, Alsop DC. Experimental design and the relative sensitivity of BOLD and perfusion fMRI. NeuroImage 2002;15:488–500. [PubMed: 11848692]

Barnett AH, Culver JP, Sorenson AG, Dale A, Boas DA. Robust inference of baseline optical properties of the human head with three-dimensional segmentation from magnetic resonance imaging. Appl. Opt 2003;42:3095–3108. [PubMed: 12790461]

Boas DA, Dale AM, Franceschini MA. Diffuse optical imaging of brain activation: approaches to optimizing image sensitivity, resolution and accuracy. NeuroImage 2004;23:S275–S288. [PubMed: 15501097]

Boxerman JL, Bandettini PA, Kwong KK, Baker JR, Davis TL, Rosen BR, Weisskoff RM. The intravascular contributions of fMRI signal change: Monte Carlo modeling and diffusion-weighted studies in vivo. Magn. Reson. Med 1995;34:4–10. [PubMed: 7674897]

Buxton RB, Wong EC, Frank LR. Dynamics of blood flow and oxygenation changes during brain activation: the balloon model. Magn. Reson. Med 1998;39(6):855–864. [PubMed: 9621908]

Cannestra AF, Pouratian N, Shomer MH, Toga AW. Refractory periods observed by intrinsic signal and fluorescent dye imaging. J. Neurophysiol 1998;80:1522–1532. [PubMed: 9744956]

Chen Y, Tailor DR, Intes X, Chance B. Correlation between near-infrared spectroscopy and magnetic resonance imaging of rat brain oxygenation modulation. Phys. Med. Biol 2003;48(4):417–427. [PubMed: 12630739]

Cox BA, Jesmanowicz AJ. Real-time (1999). Real-time 3D image registration for functional MRI. Magn. Reson. Med 1999;42:1014–1018. [PubMed: 10571921]

Dale AM. Optimal experimental design for event-related fMRI. Hum. Brain Mapp 1999;8:109–114. [PubMed: 10524601]

de Boor, C. A Practical Guide to Splines. Berlin: Springer-Verlag; 1978.

Franceschini M, Fantini S, Thompson JH, Culver JP, Boas DA. Hemodynamic evoked response of the sensorimotor cortex measured non-invasively with near-infrared optical imaging. Psychophysiology 2003;42(16):3063–3072.

Fukui Y, Ajichi Y, Okada E. Monte Carlo prediction of near-infrared light propagation in realistic adult and neonatal head models. Appl. Opt 2003;42(16):2881–2887. [PubMed: 12790436]

Gather U, Imhoff M, Fried R. Graphical models for multivariate time series from intensive care monitoring. Stat. Med 2002;21:2685–2701. [PubMed: 12228885]

Hoshi Y, Tamura M. Dynamic multichannel near-infrared optical imaging of human brain activity. J. Appl. Physiol 1993;75(4):1842–1846. [PubMed: 8282640]

Hoge RD, Atkinson J, Gill B, Crelier GR, Marrett S, Pike GB. Stimulus-dependent BOLD and perfusion dynamics in human V1. NeuroImage 1999;9:573–585. [PubMed: 10334901]

Hoge RD, Franceschini MA, Covolan RJM, Huppert T, Mandeville JB, Boas DA. Simultaneous recording of task-induced changes in blood oxygenation, volume, and flow using diffuse optical imaging and arterial spin-labeling MRI. NeuroImage 2005;25:701–707. [PubMed: 15808971]

Jasdzewski G, Strangman G, Wagner J, Kwong KK, Poldrack RA, Boas DA. Differences in the hemodynamic response to event-related motor and visual paradigms as measured by near-infrared spectroscopy. NeuroImage 2003;20:279–488.

Kleinschmidt A, Obrig H, Requardt M, Merboldt KD, Dirnagl U, Villringer A, Frahm J. Simultaneous recording of cerebral blood oxygenation changes during human brain activation by magnetic resonance imaging and near-infrared spectroscopy. J. Cereb. Blood Flow Metab 1996;16:817–826. [PubMed: 8784226]

Kwong KK, Belliveau JW, Chesler DA, Goldberg IE, Weisskoff RM, Poncelet BP, Kennedy DN, Hoppel BE, Cohen MS, Turner R, et al. Dynamic magnetic resonance imaging of human brain activity during primary sensory stimulation. Proc. Natl. Acad. Sci. U. S. A 1992;89(12):5675–5679. [PubMed: 1608978]

Lee A, Glover G, Meyer C. Discrimination of large venous vessels in time-course spiral blood– oxygen-level-dependent magnetic resonance functional neuroimaging. Magn. Reson. Med 1995;33:745–754. [PubMed: 7651109]

Li D, Waight DJ, Wang Y. In vivo correlation between blood T2* and oxygen saturation. J. Magn. Reson. Imaging 1998;8:1236–1239. [PubMed: 9848734]

Liu H, Chance B, Hielscher AH, Jacques SL, Tittel FK. Influence of blood vessels on the measurement of hemoglobin oxygenation as determined by time-resolved reflectance spectroscopy. Med. Phys 1995;22(8):1209–1217. [PubMed: 7476706]

Liu HL, Pu Y, Nickerson LD, Liu Y, Fox PT, Gao JH. Comparison of the temporal response in perfusion and BOLD-based event-related functional MRI. Magn. Reson. Med 2000;43(5):768–772. [PubMed: 10800045]

Luh W, Wong E, Bandettini P, Hyde J. QUIPSS II with thin-slice ti1 periodic saturation: a method for improving accuracy of quantitative perfusion imaging using pulsed arterial spin labeling. Magn. Reson. Med 1999;6(41):1246–1254. [PubMed: 10371458]

Ma J, Ayata C, Huang PL, Fishman MC, Moskowitz MA. Regional cerebral blood flow response to vibrissal stimulation in mice lacking type I NOS gene expression. Am. J. Physiol 1996;270:1085–1090.

MacIntosh BJ, Klassen LM, Menon RS. Transient hemodynamics during a breath hold challenge in a two part functional imaging study with simultaneous near-infrared spectroscopy in adult humans. NeuroImage 2003;20:1246–1252. [PubMed: 14568493]

Mandeville JB, Marota JJ, Ayata C, Zaharchuk G, Moskowitz MA, Rosen BR, Weisskoff RM. Evidence of a cerebrovascular postarteriole windkessel with delayed compliance. J. Cereb. Blood Flow Metab 1999;19(6):679–689. [PubMed: 10366199]

Miezin F, Maccotta L, Ollinger J, Petersen S, Buckner R. Characterizing the hemodynamic response: effects of presentation rate, sampling procedure, and the possibility of ordering brain activity based on relative timing. NeuroImage 2000;11:735–759. [PubMed: 10860799]

Mildner T, Norris DG, Schwarzbauer C, Wiggens CJ. A quantitative test of the balloon model for BOLD-based MR signal changes at 3T. Magn. Reson. Med 2001;46:891–899. [PubMed: 11675640]

Obata T, Thomas TL, Miller K, Luh WM, Wong EC, Frank LR, Buxton RB. Discrepancies between BOLD and flow dynamics in primary and supplementary motor areas: applications of the balloon model to the interpretation of BOLD transients. NeuroImage 2004;21:144–153. [PubMed: 14741651]

Ogawa S, Tank DW, Menon R, Ellermann JM, Kim SG, Merkle H, Ugurbil K. Intrinsic signal changes accompanying sensory stimulation: functional brain mapping with magnetic resonance imaging. Proc. Natl. Acad. Sci. U. S. A 1992;89(13):5951–5955. [PubMed: 1631079]

Ogawa S, Menon RS, Tank DW, Kim SG, Merkle H, Ellerman JM, Ugurbil K. Functional brain mapping by blood oxygen-level dependent contrast magnetic resonance imaging: a comparison of signal characteristics with a biophysical model. Biophys. J 1993;64:803–812. [PubMed: 8386018]

Punwani SOR, Cooper CE, Amess P, Clemence M. MRI measurements of cerebral deoxyhaemoglobin concentration [dHb]-correlation with near infrared spectroscopy (NIRS). NMR Biomed 1998;11(6): 281–289. [PubMed: 9802470]

Sato H, Kiguchi M, Kawaguchi F, Maki A. Practicality of wavelength selection to improve signal-to-noise ratio in near-infrared spectroscopy. NeuroImage 2004;21:1554–1562. [PubMed: 15050579]

Serences JT. A comparison of methods for characterizing the event-related BOLD time series in rapid fMRI. NeuroImage 2004;21:1690–1700. [PubMed: 15050591]

Siegel A, Culver JP, Mandeville JB, Boas DA. Temporal comparison of functional brain imaging with diffuse optical tomography and fMRI during rat forepaw stimulation. Phys. Med. Biol 2003;48:1391–1403. [PubMed: 12812454]

Strangman G, Culver JP, Thompson JH, Boas DA. A qualitative comparison of simultaneous BOLD fMRI and NIRS recordings during functional brain activity. NeuroImage 2002;17(2):719–731. [PubMed: 12377147]

Strangman G, Franceschini MA, Boas DA. Factors affecting the accuracy of near-infrared spectroscopy concentration calculations for the focal changes in oxygenation parameters. NeuroImage 2003;18 (4):865–879. [PubMed: 12725763]

Toronov VAW, Choi JH, Wolf M, Michalos A, Gratton E, Hueber D. Investigation of human brain hemodynamics by simultaneous near-infrared spectroscopy and functional magnetic resonance imaging. Med. Phys 2001;28(4):521–527. [PubMed: 11339749]

Toronov VAW, Walker S, Gupta R, Choi JH, Gratton E, Hueber D, Webb A. The roles of changes in deoxyhemoglobin concentration and regional cerebral blood volume in the fMRI BOLD signal. NeuroImage 2003;19(4):1521–1531. [PubMed: 12948708]

Torricelli A, Pifferi A, Taroni P, Giambattistelli E, Cubeddu R. In vivo optical characterization of human tissues from 610 to 1010 nm by time-resolved reflectance spectroscopy. Phys. Med. Biol 2001;46:2227–2237. [PubMed: 11512621]

Uludag K, Kohl M, Steinbrink J, Obrig H, Villringer A. Cross talk in the Lambert-Beer calculation for near-infrared wavelengths estimated by Monte Carlo simulations. J. Biomed. Opt 2002;7(1):51–59. [PubMed: 11818012]

Uludag K, Steinbrink J, Villringer A, Obrig H. Separability and cross talk: optimizing dual wavelength combinations for near-infrared spectroscopy of the adult head. NeuroImage 2004;22(2):583–589. [PubMed: 15193586]

Villringer A, Planck J, Hock C, Schleinkofer L, Dirnagl U. Near infrared spectroscopy (NIRS): a new tool to study hemodynamic changes during activation of brain function in human adults. Neurosci. Lett 1993;14(1– 2):101–104. [PubMed: 8361619]

Whittaker, J. Graphical Models in Applied Multivariate Statistics. Wiley, Chichester; 1990.

Wong E, Buxton R, Frank L. Implementation of quantitative perfusion imaging techniques for functional brain mapping using pulsed arterial spin labeling. NMR Biomed 1997;4– 5(10):237–249.

Worsley K, Friston K. Analysis of fMRI time-series revisited—again. NeuroImage 1995;2(3):173–181. [PubMed: 9343600]

Yamamoto T, Kato T. Paradoxical correlation between signal in functional magnetic resonance imaging and deoxygenated haemoglobin content in capillaries: a new theoretical explanation. Phys. Med. Biol 2002;47:1121–1141. [PubMed: 11996059]

Yamashita Y, Maki A, Koizumi H. Wavelength dependence of the precision of noninvasive optical measurement of oxy-, deoxy-, and total-hemoglobin concentration. Med. Phys 2001;28:1108–1114. [PubMed: 11439480]

Yang Y, E W, Pan H, Xu S, Silbersweig DA, Stern E. A CBF-based event-related brain activation paradigm: characterization of impulse-response function and comparison to BOLD. NeuroImage 2000;12(3):287–297. [PubMed: 10944411]

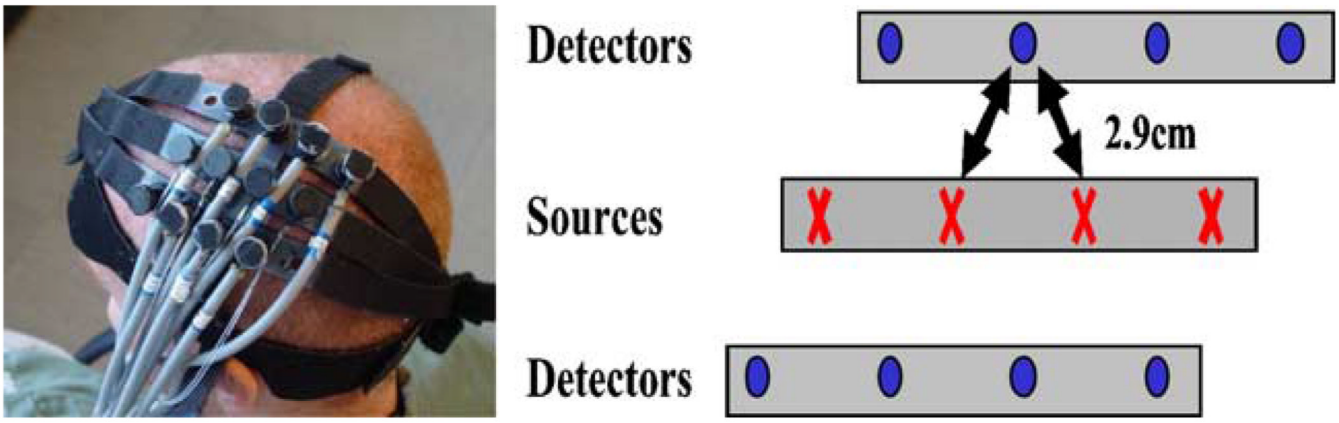

Fig. 1.

Probe design and placement for NIRS measurements. This probe consisted of 8 detector positions (most medial and lateral rows) and 4 source positions (middle row). The source detector separation was 2.9 cm. This probe was positioned approximately over the subject's contra-lateral primary motor cortex as the subject lay in the MRI scanner. The probe also contains vitamin E rings placed on the caps of the optodes, which allowed registration of the optode array in the MR structural image (shown in Fig. 2).

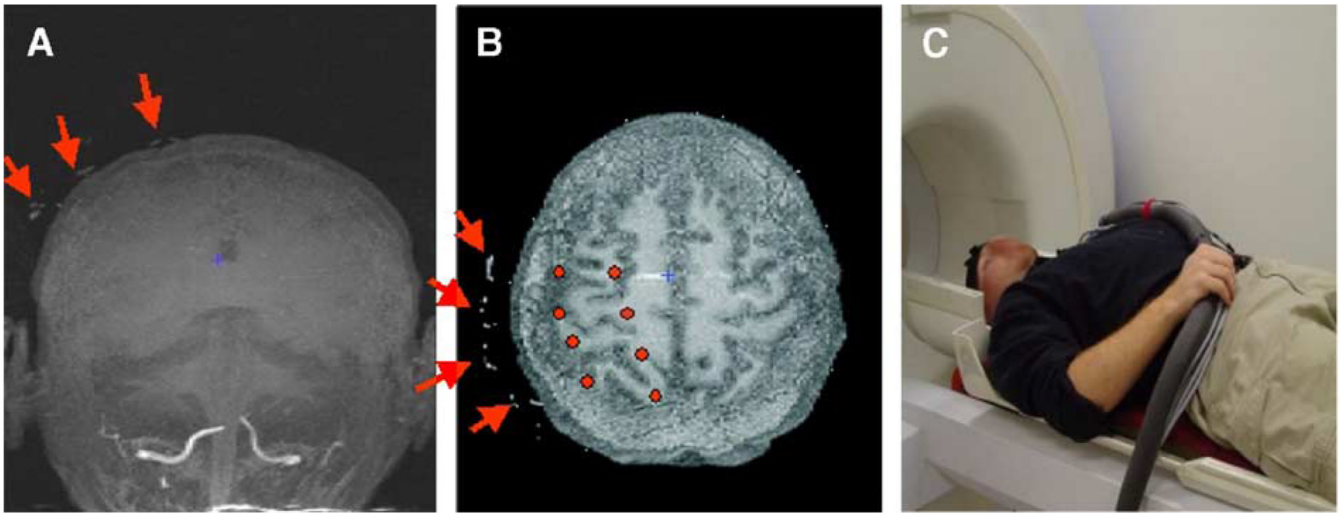

Fig. 2.

The NIRS probe placement was determined from vitamin E fiducial markers, which showed in the MPRAGE structural MR images. fMRI regions-of-interest were selected from significant ($P < 0.01$) pixels manually located under the probe. In all cases, this included all pixels within the primary motor area. Images (A and B) above show maximum intensity projections demonstrating the location of the probe on a sample subject. Image (C) shows the preparation for simultaneous acquisition of the fMRI and NIRS, demonstrating the positioned probe on a MRI subject.

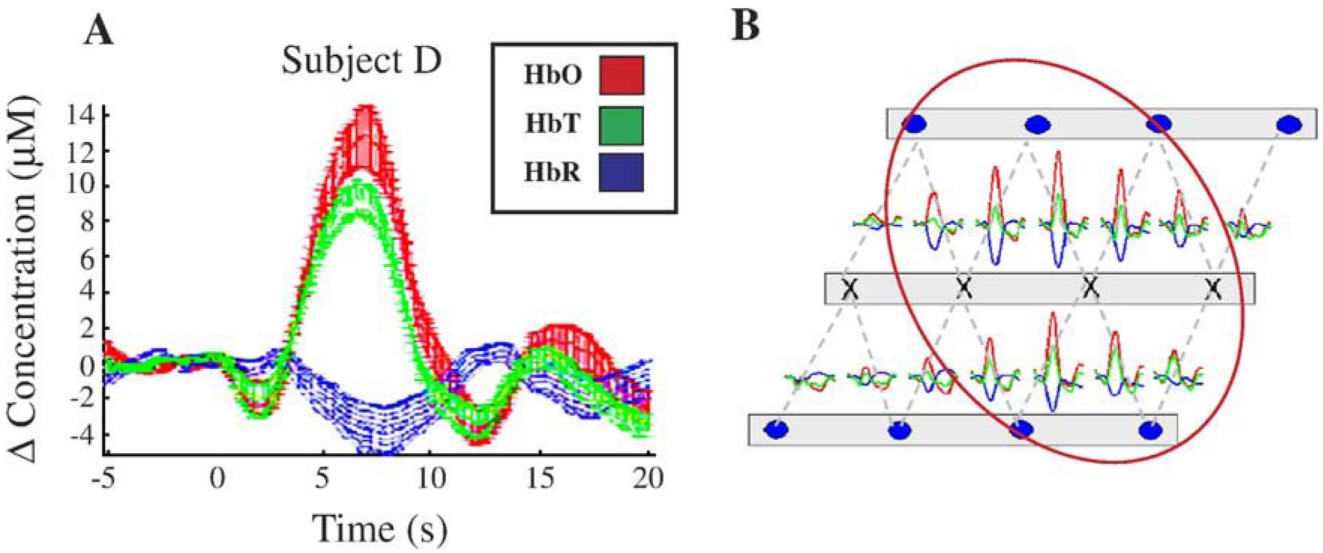

Fig. 3.

Here, we show a typical hemodynamic response for one subject as recorded by the NIRS instrument. Subplot (A) shows the region-of-interest averaged results obtained from averaging across all significant ($P < 0.01$) source detector pairs for all 6 runs. The error bars shown are the standard error across the same channels. Plot (B) shows the total array of source detector pairs that were recorded during the scan. Those that were used in the region-of-interest average are circled.

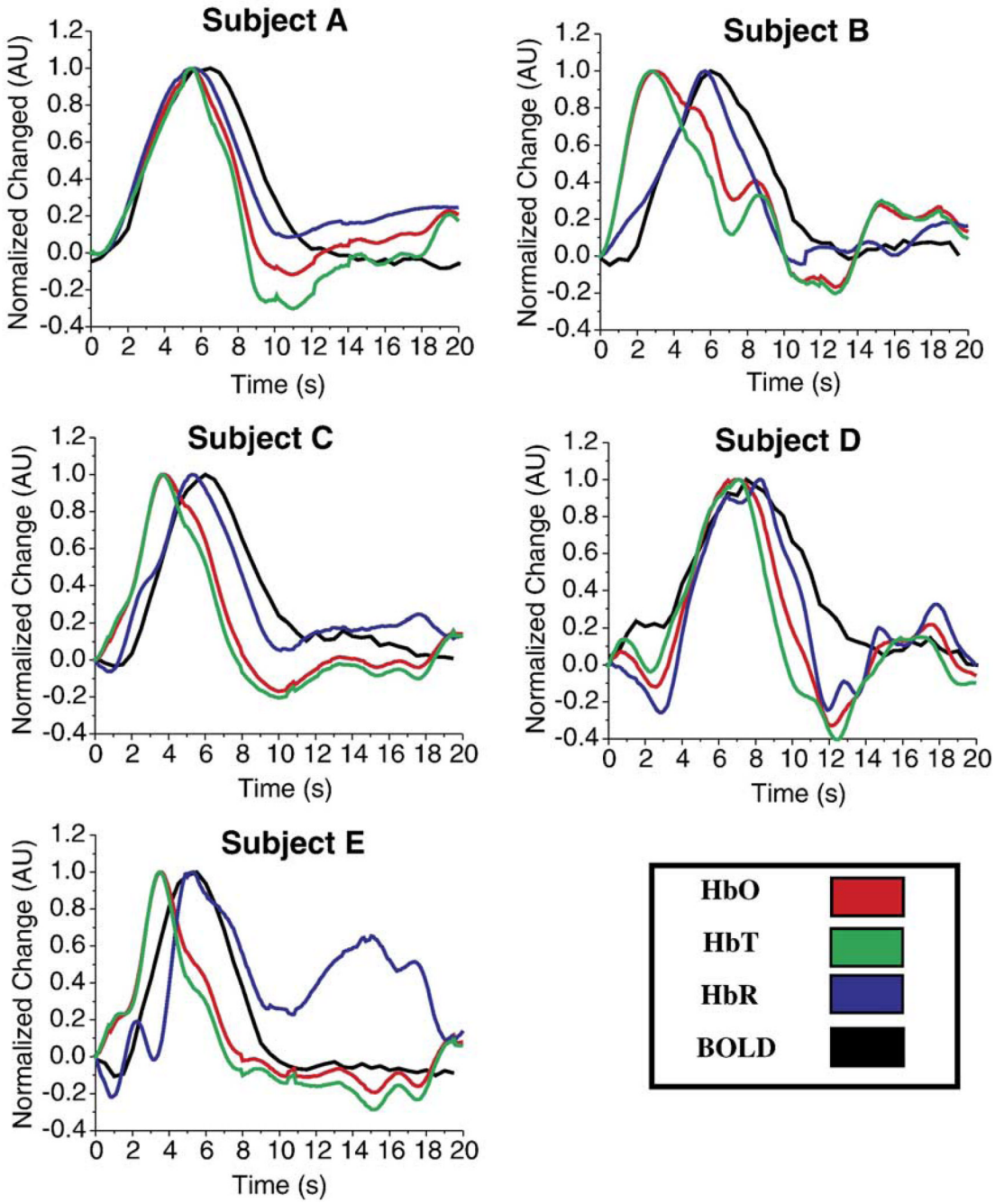

Fig. 4.

Here we display the hemodynamic response functions for each of the five individual subjects used in study I. The maximum change of each parameter has been normalized to unity and the HbR response has been inverted for comparison. In each of the five subjects, the BOLD signal closely tracks the HbR measurement.

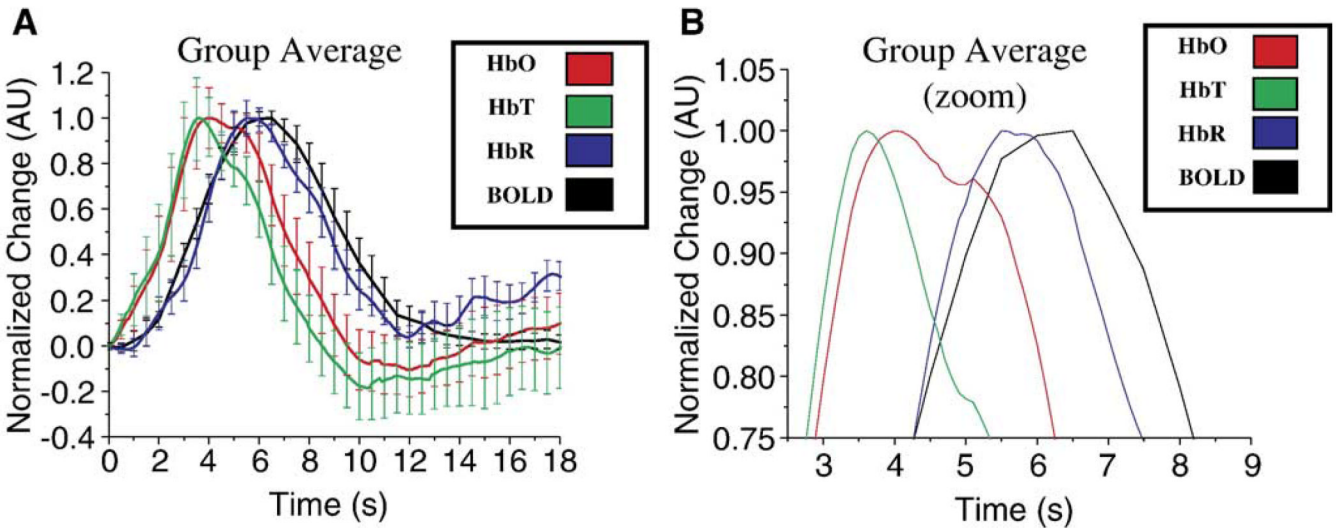

Fig. 5.

Here, we display the five subject averaged hemodynamic response function for both the NIRS and BOLD responses. Curves were calculated from the average of the five normalized responses shown in Fig. 4. Again, the maximum change has been normalized to unity and the HbR response has been inverted. The error bars on plot (A) show the standard error of each time point from this average. Plot (B) is a zoomed scaling of the same data highlighting the response peaks. Like the individual results, the BOLD signal closely tracks the HbR measurement.

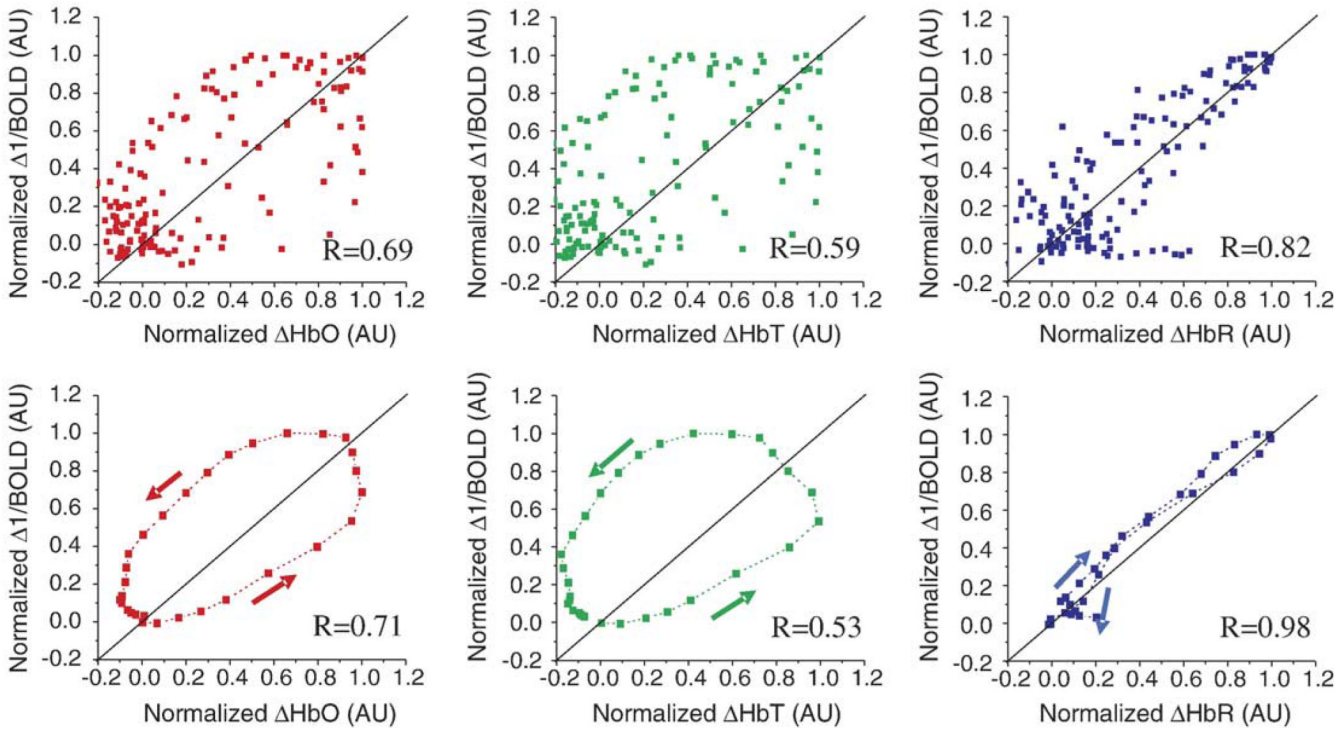

Fig. 6.

These parametric plots show the linear correlation between HbO, HbT, and HbR (from left to right) and BOLD. The plots on top represent all individual data from the five subjects. The plots on the bottom show only the subject averaged response functions. The arrows (shown only on the averaged data) indicate the direction of time in the data. The linear correlation coefficients are presented in the bottom of each plot.

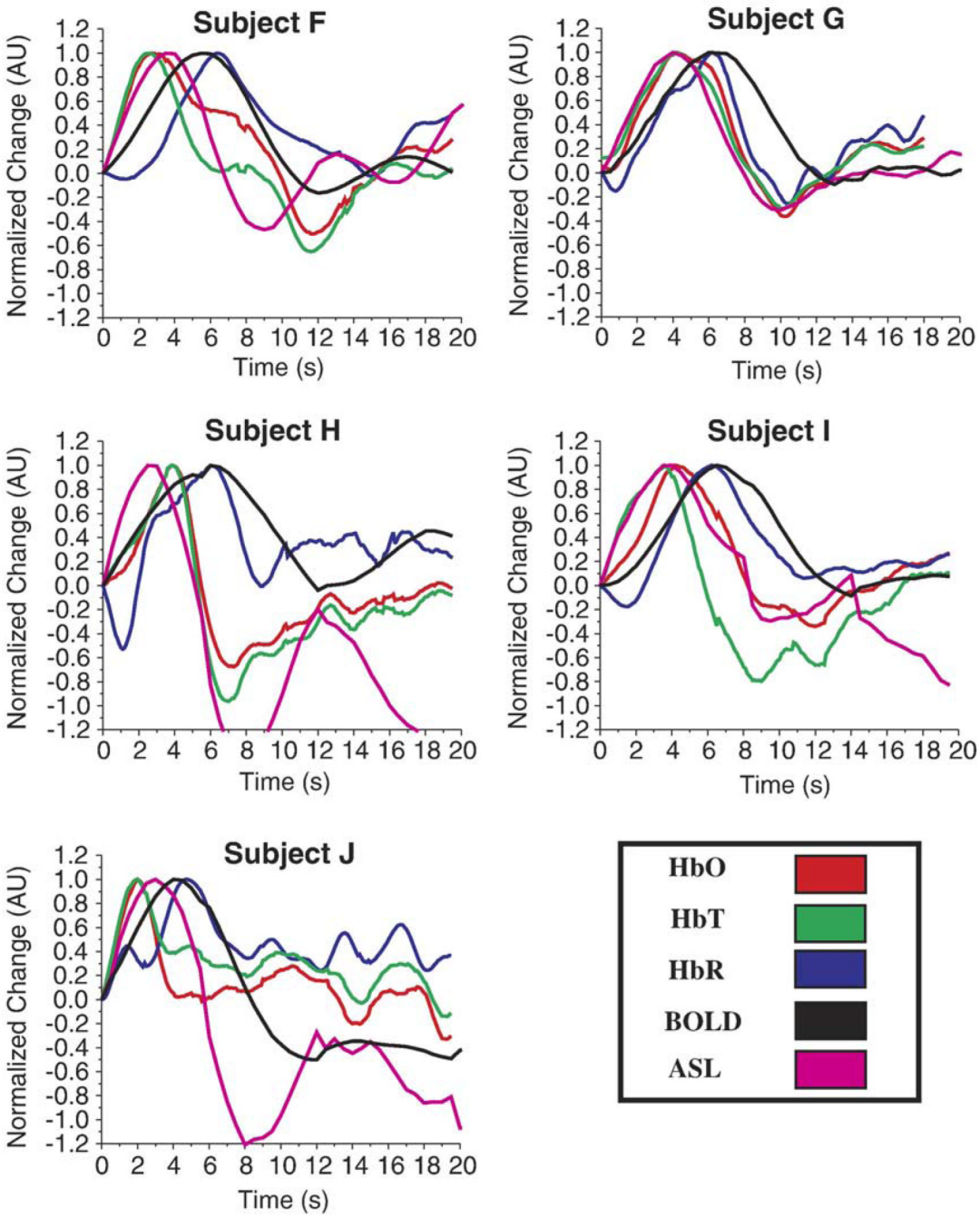

Fig. 7.

Here we display the BOLD, ASL, and NIRS hemodynamic response functions for each of the five individual subjects used in study II. The maximum change of each parameter has been normalized to unity and the HbR response has been inverted for comparison.

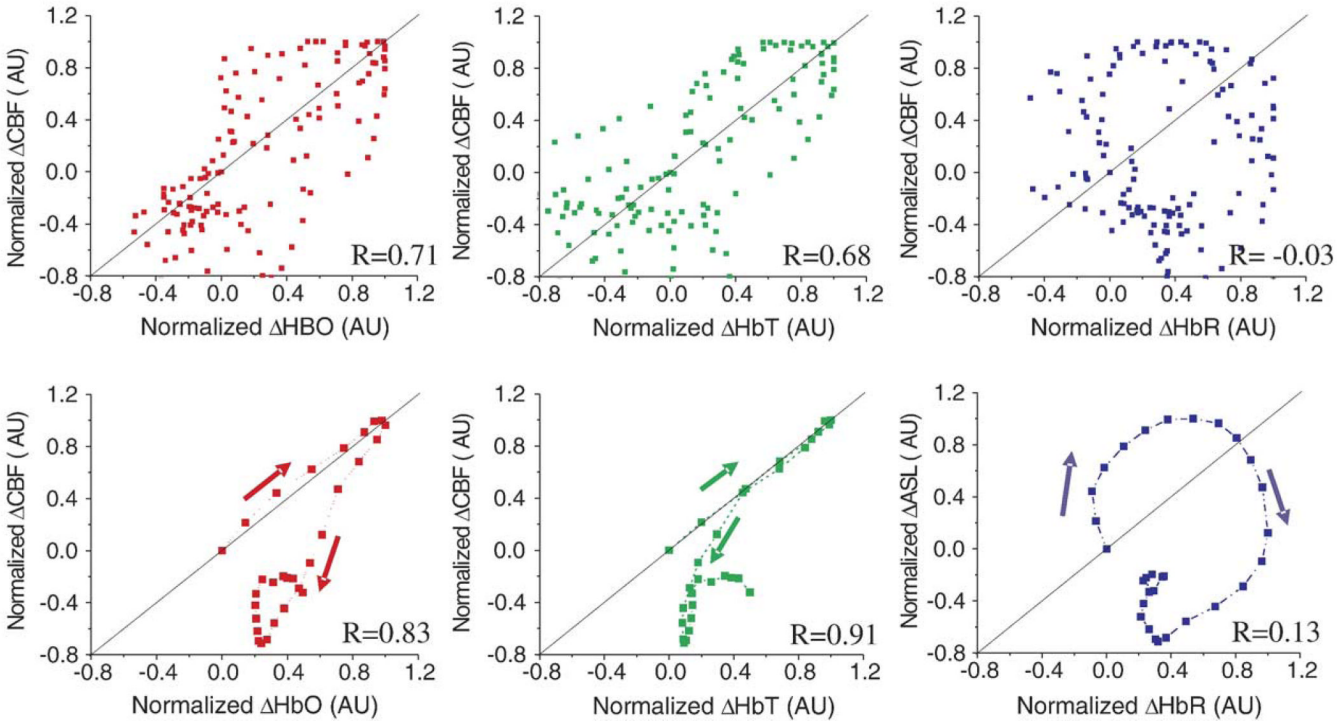

Fig. 8.

These parametric plots show the linear correlation between HbO, HbT, and HbR (from left to right) and ASL. Again, the images on top represent all individual data from the five subjects. The plots on the bottom show only the subject averaged response functions. The arrows (shown only on the averaged data) indicate the direction of time in the data. The linear correlation coefficients are presented in the bottom of each plot.

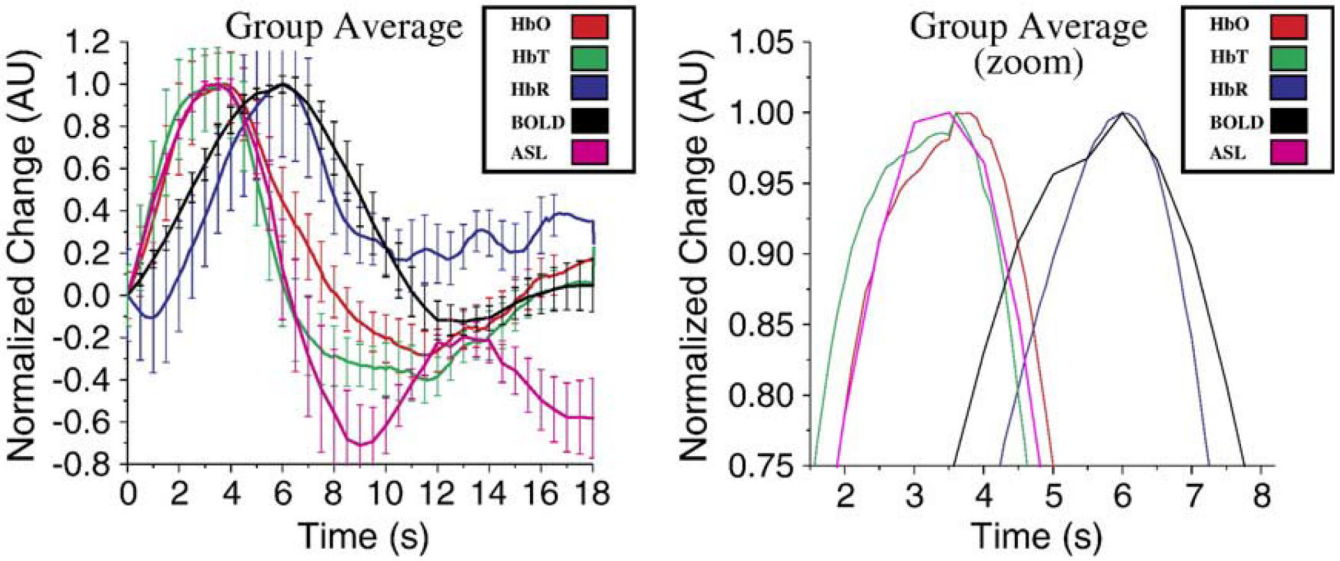

Fig. 9.

Here, we present the group averaged response functions from simultaneous NIRS and ASL-fMRI scans (study II). As was also seen in the individual subject data, the ASL measured CBF clearly peaks around 2 s earlier then the BOLD response. The NIRS measured HbT/HbO and HbR responses closely agree with the fMRI responses of CBF and BOLD respectively. The figure on the right shows a zoomed view of the same response, highlighting the clear separation in time-to-peak between the HbO:HbT:ASL and HbR:BOLD responses.

Table 1

The time to peak (seconds) of the region-of-interest averaged responses for each of the five hemodynamic parameters measured for each of the five subjects used in each study

Subject #	Time to peak (s)				
	HbO	HbT	HbR	BOLD	ASL
Study I					
A	5.5	5.4	5.5	6.5	-
B*	2.9	2.8	5.7	6	-
C	3.8	3.7	5.3	6	-
D	7.1	7.1	8.2	7.5	-
E	3.5	3.5	5.3	5.5	-
Group average	4.6 (1.7)	4.5 (1.7)	6.0 (1.2)	6.3 (0.8)	-
Study II					
F*	2.8	2.6	6.4	5.5	3.5
G	4.2	4.2	6.2	6	4
H	3.9	3.9	6	6	2.5
I	4.2	3.6	6.2	6.4	4
J	2	2	4.7	4	3
Group average	3.4 (1.0)	3.3 (0.9)	5.9 (0.7)	5.6 (0.9)	3.4 (0.7)
Average of both	4.0 (1.4)	3.9 (1.5)	6.0 (1.0)	5.9 (0.9)	3.4 (0.7)

Time-to-peak values were calculated as the time to maximum (or minimum in the case of HbR) response from the presentation of the stimulus. The average shows the mean with the standard deviation in parentheses. The temporal resolution for BOLD and ASL responses were ±500 ms and was ±100 ms for the HbO, HbT, and HbR (NIRS) measurements. Subjects B and F were the same subject repeated in both studies.

Table 2

Here, we present the zero lag correlation (Pearson's) coefficients for the three comparisons

Subject	HbO:1/BOLD	HbT:1/BOLD	HbR:1/BOLD
A	0.88 (2×10^{-10})	0.81 (7×10^{-08})	0.93 (4×10^{-14})
B	0.50 (5×10^{-03})	0.32 (9×10^{-02})	0.90 (7×10^{-12})
C	0.57 (1×10^{-03})	0.47 (9×10^{-03})	0.94 (3×10^{-14})
D	0.87 (4×10^{-10})	0.74 (3×10^{-06})	0.94 (1×10^{-14})
E	0.71 (1×10^{-05})	0.62 (3×10^{-04})	0.64 (1×10^{-04})
All	0.71 (1×10^{-05})	0.53 (2×10^{-03})	0.98 (8×10^{-21})

The values in parenthesis are the *P* values for each coefficient. For all five individual subjects, the BOLD response showed highly significant ($P < 10^{-4}$) correlation. Only one of the five subjects did not show the best correlation to be between BOLD and the HbR response. The correlations for the averaged response are presented in the bottom row. The HbR:BOLD correlation was again highly significant ($P < 8 \times 10^{-21}$). The time period from 0–15 s post-stimulus was used for all correlations.

Table 3

Here we present the zero lag correlation (Pearson's) coefficients for the six comparisons between HbX and fMRI for study II

Subject	HbO:ASL	HbT:ASL	HbR:ASL
F	0.74 (3×10^{-06})	0.81 (6×10^{-08})	−0.15 (4×10^{-01})
G	0.95 (1×10^{-15})	0.98 (1×10^{-22})	0.71 (1×10^{-05})
H	0.90 (2×10^{-11})	0.92 (4×10^{-13})	−0.15 (4×10^{-01})
I	0.93 (8×10^{-14})	0.89 (4×10^{-11})	0.30 (1×10^{-01})
J	0.50 (5×10^{-03})	0.64 (2×10^{-03})	0.19 (4×10^{-01})
ALL	0.83 (1×10^{-08})	0.91 (4×10^{-12})	0.13 (5×10^{-01})
	HbO:1/BOLD	HbT:1/BOLD	HbR:1/BOLD
F	0.80 (1×10^{-07})	0.55 (2×10^{-03})	0.75 (2×10^{-06})
G	0.63 (2×10^{-04})	0.55 (2×10^{-03})	0.78 (6×10^{-07})
H	0.14 (5×10^{-01})	0.05 (8×10^{-01})	0.57 (6×10^{-04})
I	0.50 (5×10^{-03})	−0.10 (6×10^{-01})	0.91 (4×10^{-12})
J	0.25 (2×10^{-01})	0.49 (6×10^{-03})	0.59 (6×10^{-04})
ALL	0.62 (3×10^{-04})	0.30 (1×10^{-01})	0.80 (9×10^{-08})

The values in parentheses are the *P* values for each coefficient. For all calculations, the window of 0 –15 s was used. The correlations for the group-averaged responses show a significantly better correlation between the HbT:ASL responses compared to the HbO:ASL or HbR:ASL responses. As was seen in study I, the BOLD:HbR correlations were also much more statistically significant then the other two hemoglobin measures.

Table 4

Here, we present the analysis of variance and partial correlation analysis to investigate the measurement model of the BOLD signal (Obata et al., 2004): $\Delta S/S_o = V_o[(k_1 + k_2)*(1 - q) - (k_2 + k_3)*(1 - v)]$

	A/B	ANOVA analysis		Partial correlation analysis			
		***F*(BOLD,HbT|HbR)**	**Variance distribution (HbR:HbT)**	***R*(BOLD:HbR)**	***R*(BOLD:HbR,HbT) [regression model]**	***R*(BOLD:HbT|HbR)**	***R*(BOLD:HbR|HbT)**
Study I							
A	5.6	31.2 (4×10^{-07})	(93:7)	0.93 (4×10^{-14})	0.92 (4×10^{-13})	0.25 (1×10^{-01})	0.92 (3×10^{-11})
B	1.2	217.5 (3×10^{-15})	(85:15)	0.90 (7×10^{-12})	0.95 (1×10^{-15})	0.38 (3×10^{-02})	0.92 (6×10^{-11})
C	4.8	174 (3×10^{-14})	(91:9)	0.94 (3×10^{-14})	0.97 ($<1 \times 10^{-16}$)	0.30 (7×10^{-02})	0.97 (1×10^{-15})
D	6.5	4.6 (2×10^{-02})	(99:1)	0.94 (1×10^{-14})	0.94 (1×10^{-14})	0.35 (5×10^{-02})	0.91 (1×10^{-10})
E	2.7	115.5 (2×10^{-12})	(66:34)	0.64 (1×10^{-04})	0.94 (2×10^{-14})	0.69 (8×10^{-05})	0.96 (4×10^{-15})
ALL	4.2 (1.0)	68.1 (4×10^{-10})	(89:11)	0.98 ($<1 \times 10^{-16}$)	0.98 ($<1 \times 10^{-16}$)	0.33 (4×10^{-02})	0.96 ($<1 \times 10^{-16}$)
Study II							
F	0.7	244.1 (1×10^{-15})	(50:50)	0.75 (2×10^{-06})	0.96 (2×10^{-18})	0.95 (6×10^{-13})	0.94 (6×10^{-13})
G	0.1	333.7 ($<1 \times 10^{-16}$)	(99:1)	0.78 (6×10^{-07})	0.97 (6×10^{-18})	0.12 (3×10^{-01})	0.66 (1×10^{-04})
H	8.0	0.73 (5×10^{-01})	(93:7)	0.57 (6×10^{-04})	0.59 (6×10^{-04})	0.28 (5×10^{-02})	0.69 (6×10^{-05})
I	2.1	2.9 (7×10^{-03})	(85:15)	0.91 (4×10^{-12})	0.93 (8×10^{-14})	0.34 (4×10^{-02})	0.96 (1×10^{-14})
J	1.8	6.1 (8×10^{-04})	(55:45)	0.59 (6×10^{-04})	0.62 (2×10^{-04})	0.42 (2×10^{-02})	0.48 (8×10^{-03})
All	2.6 (1.4)	162 (7×10^{-14})	(80:20)	0.80 (9×10^{-08})	0.97 (2×10^{-18})	0.40 (1×10^{-02})	0.76 (3×10^{-07})
Total	N/A	246.8 (9×10^{-16})	(64:36)	0.96 ($<1 \times 10^{-16}$)	0.97 ($<1 \times 10^{-16}$)	0.72 3×10^{-06})	0.96 ($<1 \times 10^{-16}$)

Where q and v are the normalized total HbR and HbT (volume) variables taken from the NIRS recordings and $\Delta S/S_o$ is the normalized BOLD signal change. Column 2 presents the ratio of these coefficients [$A/B = (k_1 + k_2)/(k_2 + k_3)$] and the standard error for the group average. This is not given for the average of the two studies since the echo times differed. In column 3, we show the partial analysis of variance F test value and its associated null probability. This value tests the additional variance in the BOLD response that is accounted for by adding the $\Delta HbT/HbT_O$ (v) regressor to the model already including $\Delta HbR/HbR_O$ (q). This value tested statistically probable for all subjects and group averages. Columns 6 – 8 show the full and partial Pearson's coefficients (zeroth-lag correlations) and probabilities for the BOLD signal to the full regressive model (column 6) and to HbT and HbR with the other partialled out. Partial correlation is calculated by the equation: $R(AB|C) = [R(AB - R(AC) * R(BC)]/[\sqrt{(1 - R^2(AC))} * ((1 - R^2(BC))]$ for the partial correlation of A against B controlling for C, where $R(A:B)$ is the usual Pearson's coefficient of A against B (etc.). The Pearson's coefficients for the correlation of BOLD with HbR are also given in column 5 from Table 2 and Table 3. The time period of 0– 15 s was used for all analysis. For the group averages from the individual studies and across studies, the averaged response curves were used.

Table 5

Here, we show the probability of the null hypothesis (*P* values) for the correlation between the time-to-peak and magnitude of change of the various hemoglobin parameters

	Time to peak HbO	Time to peak HbT	Time to peak HbR	Time to peak BOLD	HbO max change	HbT max change	HbR max change	HbO integrated area	HbT integrated area	HbR integrated area
Time to peak HbO	-									
Time to peak HbT	≪0.01	-								
Time to peak HbR	0.02	0.02	-							
Time to peak BOLD	0.02	0.03	0.02	-						
HbO max change	0.10	0.08	0.34	0.39	-					
HbT max change	0.75	0.66	0.91	0.99	<0.01	-				
HbR max change	<0.01	<0.01	0.02	0.04	0.03	0.48	-			
HbO integrated area	0.12	0.10	0.23	0.25	≪0.01	<0.01	0.01	-		
HbT integrated area	0.54	0.47	0.74	0.73	<0.01	≪0.01	0.31	<0.01	-	
HbR integrated area	<0.01	<0.01	0.02	0.03	0.06	0.63	≪0.01	0.02	0.44	-

We found significant ($P < 0.05$) correlation between the latency of the response peak and the overall amplitude of the response for the HbR response. We also noted a similar trend for the HbO response, but the HbT response amplitude and timing seemed to be uncorrelated ($P > 0.6$). All ten subjects were used in this analysis.